

## Electronic Supporting Information for the paper: Thermal evolution of the submonolayer near-surface alloy of ZnPd on Pd(111)

J. A. Lipton-Duffin,<sup>a</sup> J. M. MacLeod,<sup>a</sup> M. Vondráček,<sup>b</sup> K. C. Prince,<sup>c</sup> R. Rosei<sup>d</sup> and F. Rosei.<sup>a</sup>

<sup>a</sup> Center for Energy, Materials and Telecommunications (ÉMT), Institut National de Recherche Scientifique, 1650 Boulevard Lionel Boulet, Varennes, QC, Canada, J3X 1S2.

<sup>b</sup> Fyzikální ústav AV ČR, v.v.i., Na Slovance 2, 182 21 Praha 8, Czech Republic.

<sup>c</sup> Elettra-Sincrotrone Trieste S.C.p.A., Basovizza-Trieste, Italy, and CNR-IOM Laboratorio TASC, Basovizza (Trieste), I-34149, Italy.

<sup>d</sup> “Nanotechnology for Energy” Laboratory of the “Consorzio per la Fisica” c/o AREA Science Park, Trieste, Italy.

### LEED Images

Low energy electron diffraction images are presented as a function of coverage and sample annealing temperature. All images were taken with a primary beam energy of 61 eV.

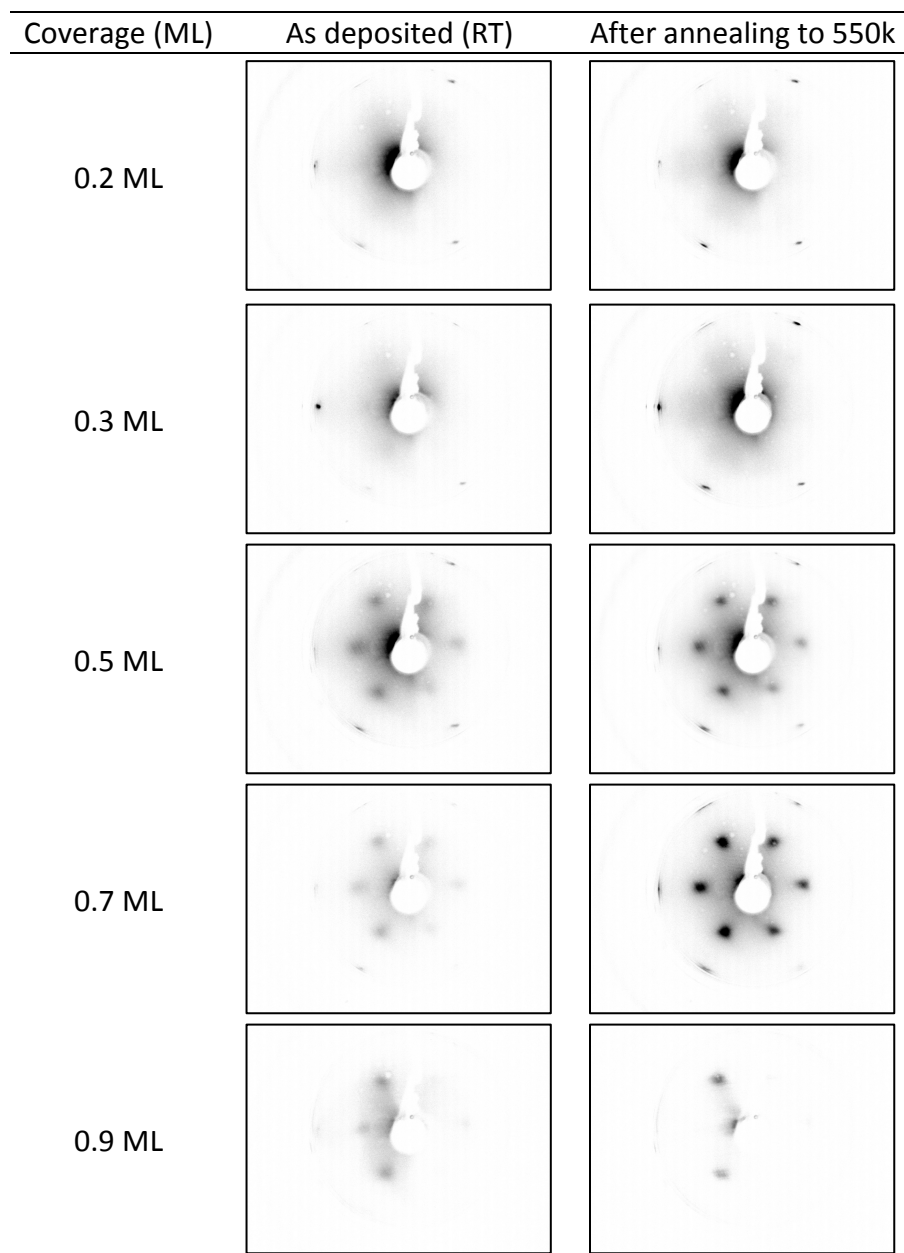


Figure S 1: LEED patterns as a function of Zn coverage and annealing.

## Details of SRPES fitting procedure

After subtracting a linear background corresponding to the low-BE profile, all SRPES data were fitted with a superposition of Doniach-Šunjić (DS) lineshapes,<sup>1</sup> an analytical function that takes into account screening by conduction electrons and their interaction with the photoelectron during its escape from the metal. It follows the form:

$$Y(E) = \cos \left[ \frac{\pi\alpha}{2} + (1 - \alpha) \tan^{-1} \left( \frac{E}{\gamma} \right) \right] (E^2 + \gamma^2)^{-\frac{(1-\alpha)}{2}},$$

where  $E$  is the energy relative to the peak maximum (at  $E=0$  in this form),  $\gamma$  is a Lorentzian-like lifetime broadening, and  $\alpha$  is an asymmetry parameter that describes the shake-up processes due to the effect of the conduction band. To account for the effects of instrumental and inhomogeneous broadening, each of the DS profiles was convoluted with a Gaussian of width  $\Gamma$ .

Thus, each of the fitted components is described by five parameters: its binding energy ( $E_B$ ), its intensity ( $I$ ), and the Lorentzian, asymmetry, and Gaussian ( $\gamma$ ,  $\alpha$ ,  $\Gamma$ ) parameters for the lineshape. To reduce the parameter space, it is assumed that the latter three components are identical for each synthetic peak within a single

spectrum. Moreover, for the Pd 3d lineshape it is assumed that these parameters are intrinsic and do not vary over the entire course of the experiment, once fixed by a rational fitting procedure for data obtained from the clean surface.

The clean surface was fit with three separate components. The detailed fits, including the lineshape parameters and  $\chi^2$  values, are shown in Figure S 2. In these particular fits, all parameters are allowed to vary freely in order to minimize the least-squares difference by the Levenberg-Marquardt algorithm. However, while the  $\gamma$ ,  $\alpha$ , and  $\Gamma$  parameters are all free to vary, they are shared between all of the separate components in each fit.

While it is clear from both the shape of the residual curve and the  $\chi^2$  values that the fitting is improved by going from a single component to two components, it is worth noting that the  $\chi^2$  value is not improved when going from a two-component fit to a three-component fit. However, it is well known that the core level spectrum of Pd(111) comprises two small surface core-level shifted (SCLS) contributions, from the surface (at lower binding energy) and the 2<sup>nd</sup>

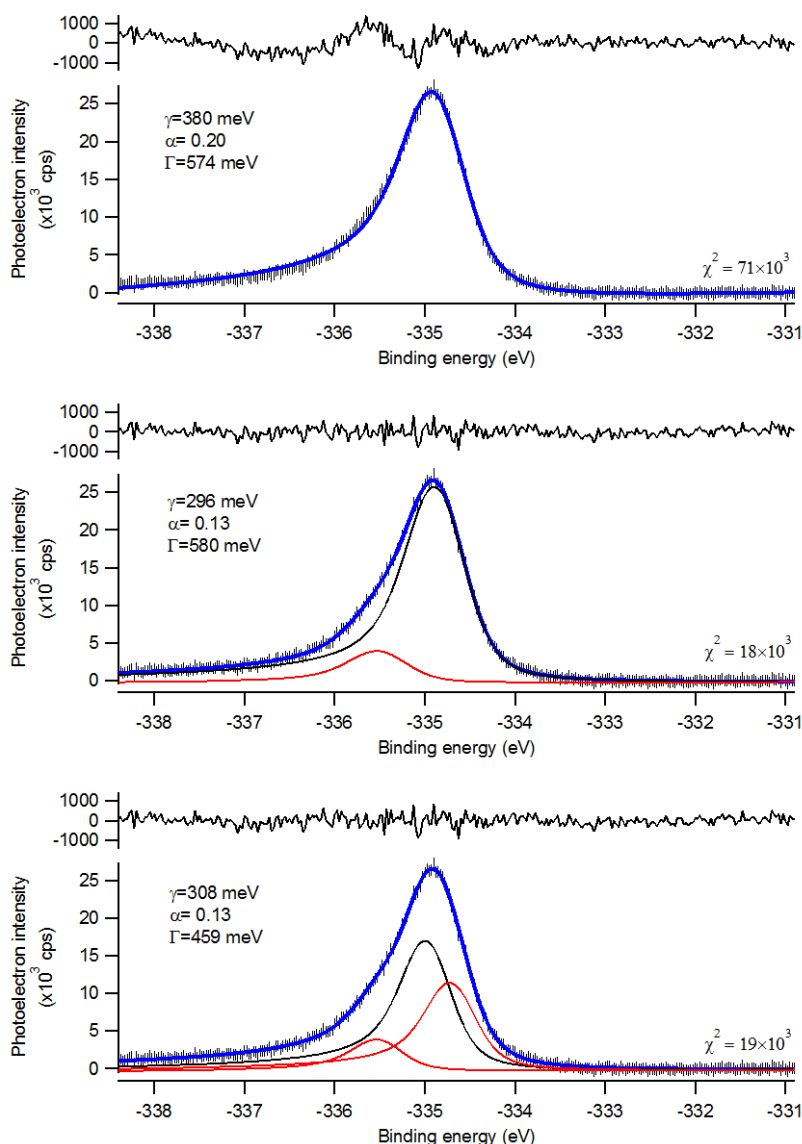


Figure S 2: Peak-fitting steps for the (clean) Pd 3d<sub>5/2</sub> core level spectrum.

layer (at higher binding energy), in addition to the dominant peak from the bulk states.<sup>2</sup> With the three-component fit we find SCLSs of -273 meV (surface) and +530 meV (2<sup>nd</sup> layer), as well as a bulk peak binding energy of -334.94 eV, all in excellent agreement with the previous study. We have therefore chosen to take the lineshape parameters derived from the three-component fit to treat all of the Pd 3d spectra.

The procedure described above is virtually identical for the fitting of the Zn 3d core level. However, there are a few key differences. The spin-orbit splitting in Zn 3d is not sufficient to treat only the 3d<sub>5/2</sub> peak in the analysis, and hence each spectrum is fit with a series of DS doublets. As with the Pd 3d data, the doublets all comprise identical  $\gamma$ ,  $\alpha$ , and  $\Gamma$  parameters, but additionally comprise two additional parameters for the spin-orbit splitting ( $\Delta_{SO}$ ) and the branching ratio ( $\beta$ ). Because of the low binding energy of the Zn 3d core level ( $\approx 9$  eV) and its susceptibility to influence by the local crystal field,<sup>3</sup> we find a larger variability in these lineshape parameters when fitting the doublets, as described in the MS text. The data were considered to be well fit when the  $\chi^2$  value was not reduced by the addition of any new identically-shaped doublets. The fits were improved by iteratively fitting the dataset, allowing parameters to vary in turn, until the  $\chi^2$  values for all spectra were below an acceptable threshold. To ensure self-consistency of the dataset, the iteration was finalized when the parameters  $\alpha$ ,  $\beta$ ,  $\gamma$  and the SCLSs were identical across all fitted spectra.

1. Doniach, S. and Šunjić, M., *Many-electron singularity in X-ray photoemission and X-ray line spectra from metals*, Journal of Physics C: Solid State Physics, **3**, 285, (1970).
2. Gladys, M. J., et al., *Chemical composition and reactivity of water on clean and oxygen-covered Pd{111}*, Surf. Sci., **602**, 3540-3549, (2008).
3. Ley, L., et al., *Crystal-field effects on the apparent spin-orbit splitting of core and valence levels observed by x-ray photoemission*, Phys. Rev. B, **10**, 4881-4888, (1974).